

High-Order Harmonic Generation in a Driven Two Level Atom: An Analogy with the Three-Step Model

C. Figueira de Morisson Faria¹ and I. Rotter²

¹ Max Born Institut für nichtlineare Optik und Kurzzeitspektroskopie, Max Born Str. 2A, 12489 Berlin, Germany
e-mail: faria@mbi-berlin.de

² Max Planck Institut für Physik komplexer Systeme, Nöthnitzer Str. 38, D-01187 Dresden, Germany
e-mail: rotter@mpipks-dresden.mpg.de

Received October 9, 2002

Abstract—We provide a summarizing account of several features which relate high-order harmonic generation in a driven two-level atom to the well-known physical picture of an electron recombining with its parent ion. The similarities observed in both models can be traced back to common physical mechanisms, namely, three-step processes, which either involve the ground state and the continuum or the adiabatic states which follow from the diagonalization of the two-level Hamiltonian. Furthermore, using scaling laws, one may extend the parameter range to a physical situation for which the two-level atom picture can be applicable, as for instance solid-state systems in strong fields.

1. INTRODUCTION

The main features of the generation of high-order harmonics of a strong laser field ($I \sim 10^{14}$ W/cm²) in gases composed of atoms or small molecules are the frequency region of harmonics of comparable intensities known as “the plateau,” followed by a drop in the harmonic yield known as “the cutoff.” Other features which are present in high-order harmonic generation (HHG) are the times at which the main contributions to this phenomenon take place and a phase difference between the fundamental and the harmonic field, which depends on the driving-field intensity. All these features are very well explained by the so-called “three-step model.” In this model, high-order harmonic generation is a consequence of a three-step process, in which an electron leaves an atom at the instant t_0 , propagates in the continuum, gaining kinetic energy from the field, and recombines with the ground state of its parent ion at a later time t_1 , releasing this kinetic energy in the form of high harmonics [1].

There is however another model that was extensively used for describing HHG until the early 1990s, namely, a driven two-level atom [2]. In this model, HHG is not a result of the interplay between the continuum and the ground state, but only bound states are involved in the process. This physical picture has been abandoned for a very simple reason: in comparison with existing experiments, the three-step model has proven to be far superior, thus establishing itself as the paradigm for the theoretical description of this phenomenon.

This is true for gaseous samples, which, until very recently, were believed to be the only systems for which HHG is feasible, due to the high intensities

involved. However, nowadays, with the advent of ultrashort pulses, there exist solid-state materials which can survive the necessary intensity regime [3]. Furthermore, alternative systems, such as thin crystals [4], carbon nanotubes [5], or larger molecules [6], have attracted considerable attention as possible high-order harmonic sources. For such materials, it is not clear whether the three-step model in its present form, in which bound-to-continuum transitions play a major role, is applicable. Thus, transitions involving solely bound states, and consequently a two-level atom, have again become of interest. Indeed, such a system is the simplest case in which population transfers between bound states occur and therefore can be taken as a starting point towards a description of HHG in more complex systems.

Of the countless studies of HHG from a two-level atom, relatively few were directly concerned with the physical mechanisms involved [7–10]. In those papers, HHG is related to abrupt population transfers between the time-dependent states, which approximately follow the field and are obtained from the diagonalization of the two-level Hamiltonian. However, in [7–9], this physical mechanism was only investigated to a limited extent.

More specifically, in [7], the emphasis lies on the existence of the plateau and how this feature depends on the adiabatic-state physical picture. It is suggested that the energy of the adiabatic states is converted into high-order harmonics, and the times for which high harmonics are generated are derived. However, the physical mechanism responsible for the population transfer to the adiabatic excited state is not discussed.

In [8], on the other hand, the population transfer from the ground adiabatic state to the excited adiabatic state is related to the existence of periodic level crossings, which occur in the presence of a laser field. Therein, it is also shown that well-separated crossings are a necessary requirement for a wide plateau. However, in [8], the times which give the main contributions to HHG remain an open problem.

Several features observed in these references, as for instance the time scales involved in the process [8] or the expressions describing population transfers between the adiabatic states [7, 9], hint at the existence of a one-to-one correspondence between the two-level atom and the three-step model. In fact, in [8, 9], such a correspondence is proposed. However, no evidence for its existence is provided.

In [10], investigating the time profile of HHG from a two-level atom, we extended the level-crossing picture and gave solid evidence for this one-to-one correspondence by analyzing its range of validity, as well as the similarities and differences between both models. Furthermore, we have shown that, knowing the three-step mechanism which occurs in the two-level atom case, the spectra can be manipulated with additional fields and, by means of scaling laws, have established sharp criteria for the invariance of the physical quantities involved. These criteria, apart from shedding additional light on the physics of the problem, permit extending the obtained results to a broader parameter range.

In the present paper, we provide selected results of [10] with a stronger emphasis on the one-to-one correspondence between the three-step model and the two-level atom. Furthermore, we include new aspects concerning the relative phase of particular harmonics as a function of the external field strength. The paper is outlined as follows. In Section 2, we recall the two-level atom features which are necessary for the subsequent discussion. The following sections are devoted to the main properties of high-harmonic generation in such a system, such as its time profile (Section 3), the above-mentioned phase (Section 4), and the scaling behavior (Section 5). Finally, in Section 6, we close the paper with some concluding remarks.

2. TWO-LEVEL ATOM

The time-dependent wave function of a two-level atom is given by

$$|\psi(t)\rangle = C_0(t)|\phi_0\rangle + C_1(t)|\phi_1\rangle, \quad (1)$$

where $C_n(t) = \langle\phi_n|\psi(t)\rangle$ denotes the overlap of the total wave function with the n th state of an arbitrary basis. The evolution of the system is given by the time-dependent Schrödinger equation [11]:

$$i\frac{d}{dt}\begin{pmatrix} C_0(t) \\ C_1(t) \end{pmatrix} = H\begin{pmatrix} C_0(t) \\ C_1(t) \end{pmatrix}, \quad (2)$$

where H is the Hamiltonian matrix, which, in the specific problem addressed in this paper, describes an atom in an external laser field. We use atomic units throughout. Depending on the problem at hand, different sets of basis states $|\phi_n\rangle$ may be required.

For the low-intensity laser field regime, the most adequate basis are the field-free states, also known as the “diabatic basis.” In this case, the Hamiltonian is given by

$$H^D = \begin{pmatrix} -\omega_{10}/2 & x_{10}E(t) \\ x_{10}E(t) & \omega_{10}/2 \end{pmatrix}, \quad (3)$$

where ω_{10} is the transition frequency between the field-free bound states, $E(t) = E_0f(t)$ is the external field, and x_{10} the dipole matrix element $\langle\phi_0^D|\hat{x}|\phi_1^D\rangle$, where $|\phi_n^D\rangle$ denotes the field-free, “diabatic” basis states.

For strong laser fields, however, such states are too strongly mixed and therefore inadequate. A more appropriate basis would be the so-called “adiabatic states,” which follow from the diagonalization of H . This basis is obtained through the unitary transformation

$$U_{D\rightarrow A} = \begin{pmatrix} \cos\chi & \sin\chi \\ -\sin\chi & \cos\chi \end{pmatrix}, \quad (4)$$

with $\chi = -1/2 \arctan(2x_{10}E(t)/\omega_{10})$. This gives

$$H^A = U_{D\rightarrow A}H U_{D\rightarrow A}^T = \begin{pmatrix} \varepsilon_-^A & 0 \\ 0 & \varepsilon_+^A \end{pmatrix}, \quad (5)$$

where the field-dressed energies are

$$\varepsilon_{\pm}^A = \pm\frac{1}{2}\sqrt{\omega_{10}^2 + (2x_{10}E(t))^2}. \quad (6)$$

The adiabatic states are given by

$$|\phi_0^A(t)\rangle = \cos\chi|\phi_0^D\rangle + \sin\chi|\phi_1^D\rangle, \quad (7)$$

$$|\phi_1^A(t)\rangle = -\sin\chi|\phi_0^D\rangle + \cos\chi|\phi_1^D\rangle, \quad (8)$$

whose energies are, respectively, ε_-^A and ε_+^A . In this basis, according to Eq. (6), crossings are avoided when $E(t_0) = 0$ and, outside this region, the energies “follow” the field. If the field is strong enough, the avoided crossings are well-separated and, to first approximation, one may assume that they take place instantaneously at t_0 .

At such crossings, abrupt population transfers from $|\phi_0^A(t)\rangle$ to $|\phi_1^A(t)\rangle$ and vice versa occur. Such population transfers are related to high-order harmonic generation.

In order to compute the harmonic spectra, one needs the Fourier transform of the time-dependent dipole. This quantity is given, in its length and acceleration form, by

$$x = x_{10}[g(t)\cos 2\chi + h(t)\sin 2\chi] \quad (9)$$

and

$$\begin{aligned} \dot{x} = & -\omega_{10}^2 x + 2\omega_{10} x_{10}^2 E(t) \\ & \times [h(t)\cos 2\chi - g(t)\sin 2\chi], \end{aligned} \quad (10)$$

with $g(t) = C_0^{*A}(t)C_1^A(t) + C_1^{*A}(t)C_0^A(t)$ and $h(t) = |C_0^A(t)|^2 - |C_1^A(t)|^2$, where $C_n^A(t) = \langle \phi_n^A(t) | \psi(t) \rangle$ denotes the projection of the wave function $|\psi(t)\rangle$ onto an adiabatic state. The above-stated equations are the superposition of two distinct terms, namely, the crossed terms and the population difference between the adiabatic states. The population difference $h(t)$ roughly follows the field, contributing mainly to the generation of low harmonics, whereas $g(t)$ yields the high-order harmonics.

In the results that follow, we use the dipole in its acceleration form and consider a monochromatic field

$$E(t) = E_0 \sin(\omega t). \quad (11)$$

Unless stated otherwise, the field is turned on immediately.

3. TIME PROFILE

Within the three-step model framework, there exist specific times for which the main contributions to HHG within a field cycle take place. They are given by the times t_1 at which the electron returns to the ground state of its parent ion. If there is a one-to-one correspondence between this model and the two-level atom, one expects a similar time profile for HHG in the latter case.

In order to extract these times from the time-dependent dipole acceleration $\dot{x}(t)$, we perform a Fourier transform of this quantity with a temporally restricted window function of Gaussian shape (the Gabor transform) given by

$$\begin{aligned} & \overline{\mathcal{F}}(t, \Omega, \sigma) \\ & = \int_{-\infty}^{+\infty} dt' \dot{x}(t') \exp[-(t-t')^2/\sigma^2] \exp[i\Omega t'], \end{aligned} \quad (12)$$

where t , Ω , and σ denote the time and harmonic frequency at which the window function is centered and its temporal width, respectively. By taking $\sigma \rightarrow \infty$,

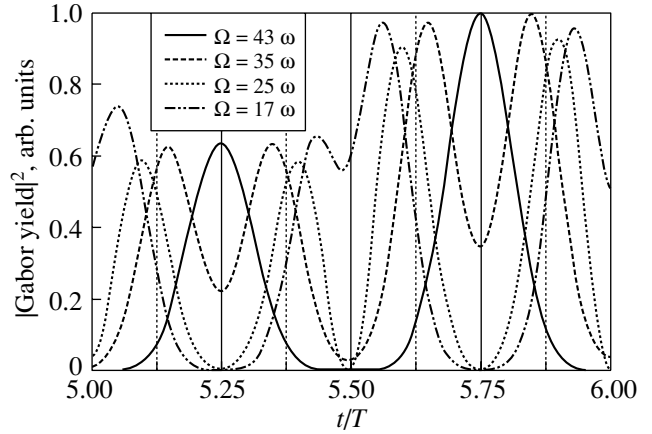


Fig. 1. Gabor spectra of the dipole acceleration (Eq. (10)) as a function of time for field strength $E_0 = 1$ a.u., field frequency $\omega = 0.05$ a.u., transition frequency $\omega_{10} = 0.409$ a.u., and dipole matrix element $x_{10} = 1.066$ a.u. These parameters give $\gamma_1 = 0.0235$ and $\gamma_2 = 0.192$. The cutoff harmonic lies at $\Omega_{\max} = 2\epsilon_{\max} = 43\omega$. The time width of the window function was chosen to be $\sigma = 0.1T$, and its center was chosen at the cutoff harmonics, as well as at harmonic energies which roughly correspond to $\Omega = 0.8\Omega_{\max}$, $\Omega = 0.6\Omega_{\max}$, and $\Omega = 0.4\Omega_{\max}$. All time-resolved spectra have been normalized. The times are given in units of the field cycle $T = 2\pi/\omega$.

one recovers the usual Fourier transform $\overline{\mathcal{F}}(\Omega)$, which does not contain any temporal information. For a temporal width smaller than the period $T = 2\pi/\omega$ of the driving field, the peaks in the time-resolved spectra $|\overline{\mathcal{F}}(t, \Omega, \sigma)|^2$ yield the recombination times t_1 . The temporal width σ corresponds to a frequency bandwidth $\sigma_{\Omega} = 2/\sigma$.

Within the three-step model framework, the Gabor transform has proven to be very useful to draw a physical picture of HHG [12, 13]. In the following, this method will be applied to the two-level atom. We choose the field and atomic parameters in such a way that the avoided crossings are well separated. For a monochromatic field, such crossings occur at the times $t_0 = n\pi/\omega$ for which the field is vanishing.

The time profile of such harmonics is displayed in Fig. 1. In this figure, the center of the window function is displaced from the cutoff to the plateau harmonics with decreasing harmonic energy. When the window function is centered at the cutoff harmonic, there exists a single peak at the times for which the field is maximal. As the center of the window function is moved into the plateau region, this peak splits into two. The lower the harmonic order is, the farther apart such peaks are. This pattern can be interpreted as following: at the times the level crossings occur, i.e., at $t_0 = nT/2$, there is population transfer from the adiabatic state $|\phi_0^A(t)\rangle$ to $|\phi_1^A(t)\rangle$, where the system remains until a further time

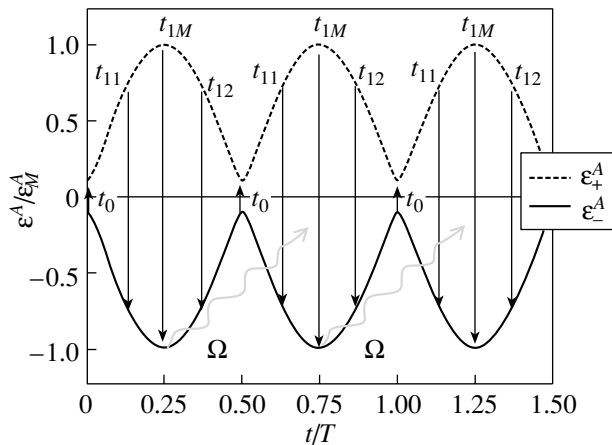


Fig. 2. Schematic representation of high-harmonic generation in a two-level atom. The population transfers at the level crossings occur at the times t_0 , and the main contributions to HHG occur at the times t_1 . The times t_{1M} , t_{11} , and t_{12} correspond to the generation of the cutoff and plateau harmonics, respectively. The main physical processes are indicated by arrows in the figure, and the corresponding energies can be read in the vertical axis. The times are given in units of the field cycle, and the energies, in units of the cutoff energy.

t_1 . At this time, the system decays back to $|\phi_0^A(t)\rangle$, emitting a harmonic of frequency $\Omega = N\omega = \varepsilon_+^A - \varepsilon_-^A$.

The times t_1 are explicitly given by

$$\omega t_1 = \arcsin[\pm\sqrt{(N\gamma_1)^2 - (\gamma_2)^2}], \quad (13)$$

with $\gamma_1 = \omega/(2x_{10}E_0)$ and $\gamma_2 = \omega_{10}/(2x_{10}E_0)$. The maximal harmonic energy (i.e., the cutoff harmonic) is obtained for the times for which the energy difference $\varepsilon_+^A - \varepsilon_-^A$ is maximal. This occurs at the times for which $E(t)$ is maximal, i.e., at $t_{1M} = (2n + 1)\pi/2\omega$. With decreasing harmonic energy, according to Eq. (13), there exist two possible times for which this population transfer occurs, a shorter and a longer one. If the harmonic energies are close to the transition frequency ω_{10} , the times t_1 , as expected, are close to the level-crossing times t_0 . This process repeats itself every half a period of the laser field. These results are in agreement with those obtained in [7] by using the saddle-point method.

A similar time profile occurs in the three-step model framework. For the cutoff harmonic, there is a single set of return times which corresponds to the maximal kinetic energy of the electron upon return. This set of times splits into two in the plateau region, the peaks getting further apart as the harmonic energy decreases [12]. This is a clear sign that a one-to-one correspondence between both models exists.

Indeed, the time profile observed in Fig. 1, in comparison with the results discussed in the literature [12], hints at similar physical mechanisms in both models, namely, three-step processes. Specifically, for the two-level atom case, the first step is the population transfer from $|\phi_0^A(t)\rangle$ to $|\phi_1^A(t)\rangle$ at the level-crossing times, the second step is the system following the field adiabatically in $|\phi_1^A(t)\rangle$ and gaining energy from it, and the third step is the system decaying back to $|\phi_0^A(t)\rangle$, with consequent high-order harmonic generation. A schematic representation of this process is shown in Fig. 2.

There exist however differences between the two models. For the two-level atom, the peaks in the Gabor spectra, for the cutoff harmonics, occur at the times for which the field is maximum. As the harmonic frequency decreases, the time profile gives sets of peaks around these times. In contrast to this case, for the three-step model, the cutoff return time t_{1M} is close to the times for which the field is minimum [13]. The splitting of the peaks in the time-resolved spectra occurs around these times.

A further difference is the cutoff law, which, in the three-step model, is proportional to the field intensity and not to its strength. This is due to the fact that, in this case, the essential quantity, which is converted into high-harmonic radiation, is the electron kinetic energy upon return, proportional to the intensity of the external field [1]. In the two-level atom, however, the quantity of interest is the energy difference $\varepsilon_+^A - \varepsilon_-^A$ between the adiabatic states, proportional to the field strength.

4. HIGH-ORDER HARMONIC PHASE

It is a well-known fact that high-order harmonics generated in atoms are not in phase with the driving field. This phase difference has been extensively investigated and turned out to be very important for describing the propagation of such harmonics in a macroscopic medium, e.g., a gaseous sample [14–16]. Within the three-step model physical picture, such a difference is directly related to the fact that there is a time delay between the instant the electron tunnels out and the instant it recombines and to the existence of specific tunneling and recombination times. Since, for a two-level atom, there is a difference between the level-crossing time t_0 and the high-order harmonic generation time t_1 , one also expects a phase shift between the fundamental and the high harmonics.

The time-dependent dipole, which gives the response of an atom to an intense laser field, is periodic and thus can be expanded in a Fourier series:

$$d(t) = \sum d_{n\omega} \sin(n\omega t + \theta_n(I)), \quad (14)$$

where θ_n is the intensity-dependent phase. Using the orthogonality relations of the Fourier series, this phase can be written as

$$\begin{aligned} & \theta_n(I) \\ &= \arctan[\text{Im}[d(\Omega = n\omega)]/\text{Re}[d(\Omega = n\omega)]], \end{aligned} \quad (15)$$

where $d(\Omega = n\omega)$ is the Fourier transform of the dipole moment at the n th harmonic.

We will now discuss the phase θ_n as a function of the intensity and the field strength, establishing a parallel to the three-step model. In the framework of the three-step model, this phase is roughly proportional to the intensity multiplied by the excursion time of the electron in the continuum [15]. In the two-level atom case, as a major difference from the three-step model, one expects the phase to be proportional to the field strength instead of the intensity.

This can be understood as follows. The part of the wave function related to the population, which, at t_0 , is transferred from $|\phi_0^A(t_0)\rangle$ to $|\phi_1^A(t_0)\rangle$ and which is responsible for HHG, is proportional to $|\phi_1^A(t)\rangle$. This wave function will be denoted $|\psi_h(t)\rangle$. In the time interval $\tau = t_1 - t_0$ from the level-crossing time t_0 to the population-transfer time t_1 , the time evolution of $|\psi_h(t)\rangle$ is given by

$$|\psi_h(t_1)\rangle \sim \exp\left[i\int_{t_0}^{t_1} H(t)dt\right]|\phi_1^A(t)\rangle. \quad (16)$$

Thus, the system ‘‘picked up’’ the phase

$$\theta_n \sim i\int_{t_0}^{t_1} \sqrt{\omega_{10}^2 + (2x_{10}E(t))^2} dt, \quad (17)$$

with t_1 such that the harmonic frequency Ω is given by the condition $\Omega = n\omega = \varepsilon_+^A - \varepsilon_-^A$ (Eq. (13)). More detailed studies of this dependence, as well as of the limitations of this picture, are in progress [18].

5. SCALING LAWS

The populations of the adiabatic states, and consequently the dipole acceleration, exhibit global structures, in addition to the pattern which is periodic in half a cycle of the driving field and which initiates the high harmonics [19]. Such patterns repeat themselves over a large number of periods and strongly influence the substructure of the spectra. Furthermore, they are extremely sensitive towards small changes in the field or atomic parameters. For this reason, it is of interest to find which combinations of E_0 , ω , ω_{10} , and x_{10} yield

similar spectra, i.e., with the same number of harmonics and the same substructure.

The answer to this question not only sheds considerable light on the physics of the system but, in addition, allows us to extend our results to a more realistic parameter range. Indeed, for HHG in atoms, the two-level atom is more of academic interest, since it is not experimentally feasible. This is due to the fact that, in order to obtain well-separated crossings, it would be necessary to consider frequencies and intensities for which an atom would immediately ionize. This may not be so for solid-state systems, as for instance quantum wells subject to external fields [9, 20].

In Eq. (13), which relates the harmonic energy to the energy difference of the adiabatic states, the field and atomic parameters always appear combined as $\gamma_1 = \omega/(2x_{10}E_0)$ or $\gamma_2 = \omega_{10}/(2x_{10}E_0)$. Thus, if these parameters remain invariant, the spectra are expected to keep the same characteristics.

This can be shown in a more systematic way, using scaling laws which have been derived elsewhere, in the context of atomic stabilization in strong laser fields [21]. Such laws are based on the requirement that the Schrödinger equation remains invariant. Let us consider the scaling transformation

$$\omega \longrightarrow \omega' = \lambda\omega; \quad \omega_{10} \longrightarrow \omega'_{10} = \lambda\omega_{10}; \quad (18)$$

$$\Omega_R \longrightarrow \Omega'_R = \lambda\Omega_R,$$

where λ denotes the dilatation factor and $\Omega_R = 2x_{10}E_0$ is the Rabi frequency, which scales like the energies. The invariance of the Schrödinger equation also requires that the time scales as $t \longrightarrow t' = \lambda^{-1}t$, such that Eq. (13) will remain invariant. This also holds for the unitary transformation (4) which gives the adiabatic states, since it depends on E_0 , ω , ω_{10} , and x_{10} only through γ_1 and γ_2 . Thus, the populations of these states, i.e., $|C_n^A(t)|^2 = |C_n^A(t')|^2$, also remain invariant.

Figure 3 illustrates this fact. This figure displays the populations $|C_n^A(t)|^2$ of the adiabatic states, as well as the dipole acceleration, as functions of the time $\tilde{t} = \omega t/(2\pi)$, given in terms of the field cycle, for two completely different sets of parameters, which, however, keep γ_1 and γ_2 invariant. The first set of parameters is characteristic of an atom, whereas the second set of parameters is typical for quantum wells [20].

The populations of the adiabatic states are identical in both cases, and the shape of the dipole acceleration is also similar, with, however, a strong intensity drop in the solid-state case. This is expected, since the dipole acceleration scales as the dipole moment multiplied by the square of the energy [cf. Eq. (10)]. The dipole

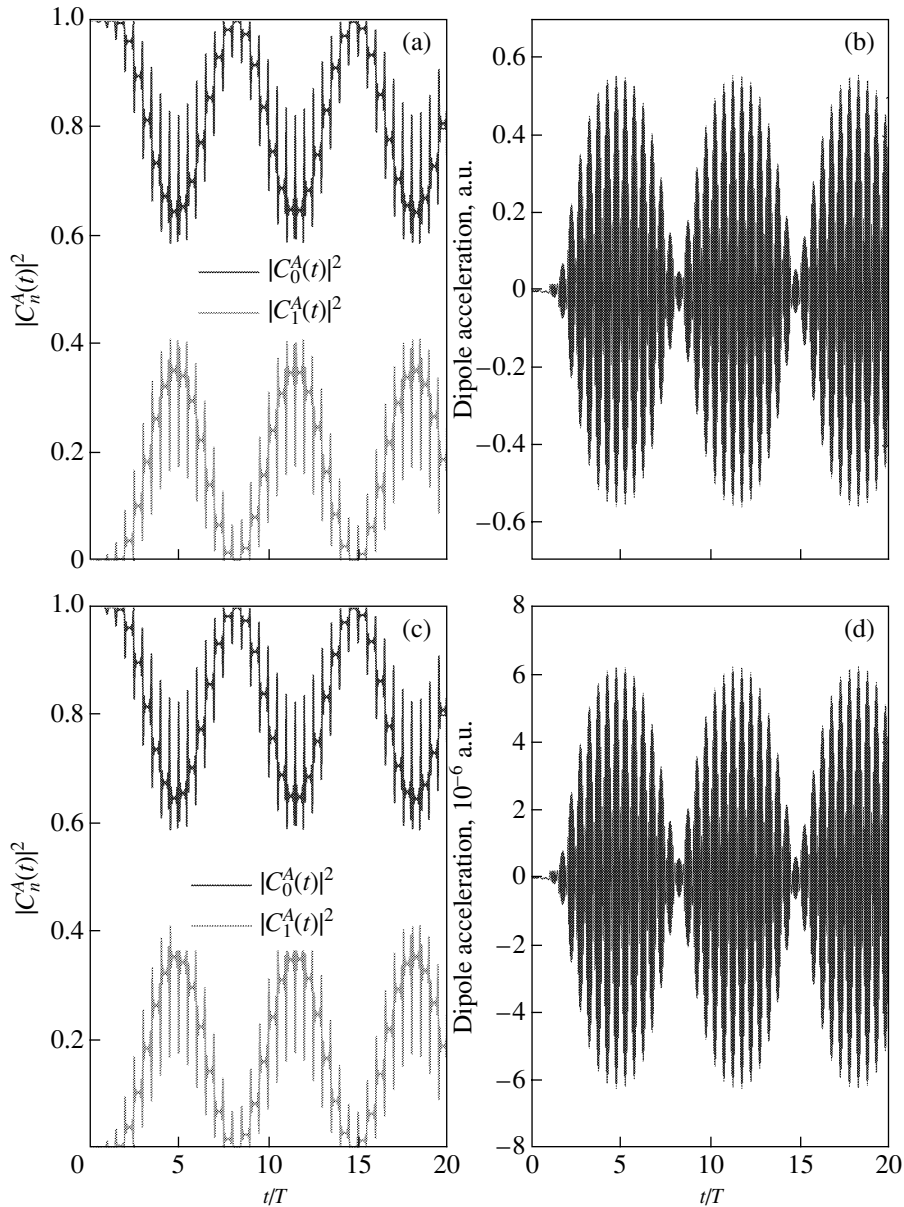


Fig. 3. Global structures as functions of time for the populations $|C_n^A(t)|^2$ (parts (a), (c)) and the dipole acceleration $\ddot{x}(t)$ (parts (b), (d)). In parts (a) and (b), the field frequency, the transition frequency, and the dipole matrix element were chosen as $E_0 = 0.6$ a.u., $\omega = 0.05$ a.u., $\omega_{10} = 0.409$ a.u., and $x_{10} = 1.066$ a.u., respectively. These parameters give $\gamma_1 = 0.0391$, $\gamma_2 = 0.3197$, and a cutoff frequency at $\Omega_{\max} = 27\omega$. In parts (c) and (d), these parameters were taken as $E_0 = 6.71 \times 10^{-6}$ a.u., $\omega = 2.5 \times 10^{-5}$ a.u., $\omega_{10} = 2.045 \times 10^{-5}$ a.u., and $x_{10} = 47.673$ a.u., respectively. These parameters are typical for solid-state systems and give the same γ_1 and γ_2 as in the previous parts. They are obtained from the previous ones using a scaling transformation with $\lambda = 1/2000$. The times are given in units of the field cycle. The field is switched on linearly within two cycles.

matrix element scales as $x_{10} \rightarrow x'_{10} = \lambda^{-1/2}x_{10}$, such that $\ddot{x}(t) \rightarrow \ddot{x}'(t') = \lambda^{3/2}\ddot{x}(t)$.

This effect influences the overall harmonic intensities in the resulting spectra. Nevertheless, the shape of such spectra, i.e., the number of harmonics, as well as their substructure, remains identical. This is shown in Fig. 4, where spectra computed for different sets of

parameters, which, however, keep γ_1 and γ_2 invariant, are displayed.

On the other hand, the extreme sensitivity of the harmonic spectra with respect to these quantities is shown in Fig. 5. In the figure, slightly different parameters yield distinct spectra due to the fact that γ_1 and γ_2 do not remain invariant.

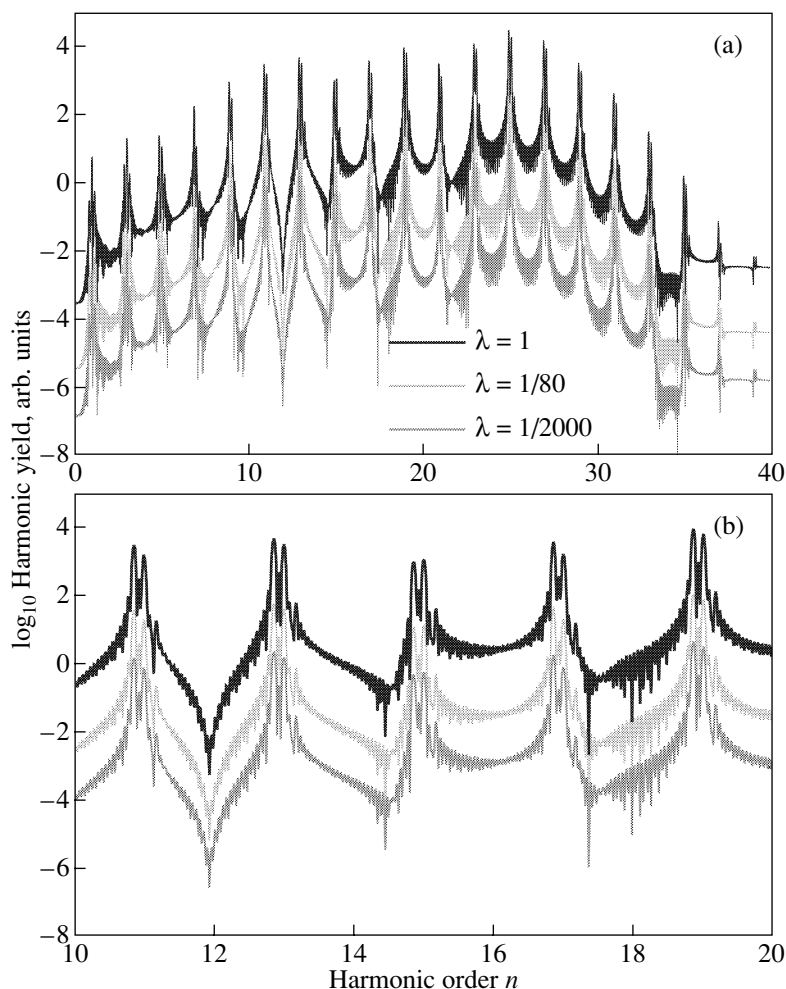


Fig. 4. Harmonic spectrum for the same parameters as in parts (a) and (b) of the previous figure (dilatation factor $\lambda = 1$) compared to those obtained for several field strengths E_0 , field frequencies ω , transition frequencies ω_{10} , and matrix dipole elements x_{10} , chosen such that $\gamma_1 = 0.0391$ and $\gamma_2 = 0.3197$ and obtained through scaling transformations (18). Part (a) shows the whole spectra, whereas part (b) displays both spectra for harmonic order $10 < N < 20$, such that their substructure can be seen. The field is switched on linearly within two cycles.

6. CONCLUSIONS

In the previous sections, we discussed some of the features analyzed in [10] in a more compact way for high-order harmonic generation in a two-level atom in a strong laser field. These features are the time profile of the high-order harmonics and the scaling properties of the physical quantities involved. Additionally, we address the phase difference between the high-order harmonics and the incident laser field. We concentrate on the similarities between the two-level atom and the three-step model, which has established itself as the paradigm for describing high-order harmonic generation in atoms.

Such similarities are clear evidence against the common belief that the three-step model and the two-level atom are completely different physical pictures. Indeed, in both cases, high-order harmonic generation

takes place as the result of a three-step process. The main difference between both models is in the relevant states. In the three-step model, they are the ground state and the continuum. In the two-level atom, they are the adiabatic states, obtained by diagonalizing the corresponding Hamiltonian.

In the three-step model case, an atom is ionized at the instant t_0 (the “first step”); propagates in the continuum, being accelerated by the field (the “second step”); and, subsequently, recombines with the ground state at a time t_1 (the “third step”), when the kinetic energy acquired in the continuum is converted into high-order harmonic radiation.

Within the two-level atom physical picture, an atom is initially in the ground adiabatic state $|\phi_0^A(t)\rangle$. At the avoided crossing time t_0 , there is population transfer

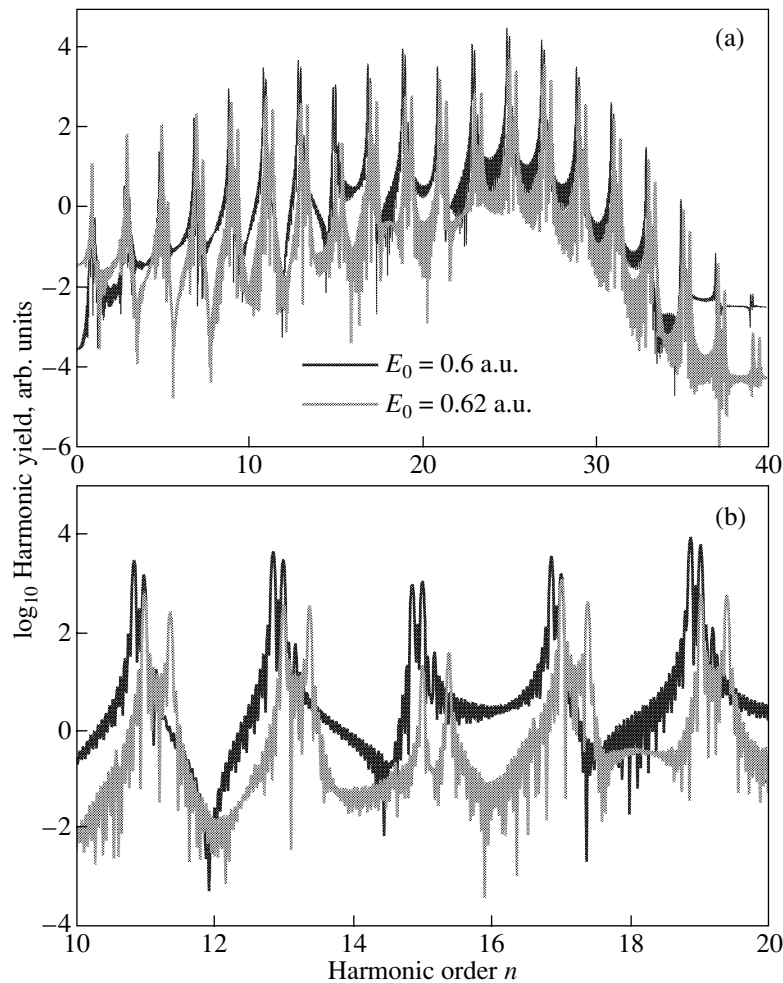


Fig. 5. Harmonic spectrum for $E_0 = 0.6$ a.u., $\omega = 0.05$ a.u., $\omega_{10} = 0.409$ a.u., and $x_{10} = 1.066$ a.u. compared to that obtained for $E_0 = 0.62$ a.u., $\omega = 0.05$ a.u., $\omega_{10} = 0.409$ a.u., and $x_{10} = 1.066$ a.u., respectively. The latter set of parameters gives $\gamma_1 = 0.0378$ and $\gamma_2 = 0.3094$, whereas the former set yields $\gamma_1 = 0.0391$ and $\gamma_2 = 0.3197$. Part (a) shows the whole spectra, whereas part (b) displays both spectra for harmonic order $10 < N < 20$, such that their substructure can be seen. The field is switched on linearly within two cycles.

from $|\phi_0^A(t)\rangle$ to the excited adiabatic state $|\phi_1^A(t)\rangle$ (the first step). Subsequently, the system remains in $|\phi_1^A(t)\rangle$, gaining energy from the field (the second step), and decays back to $|\phi_0^A(t)\rangle$ at t_1 , converting this energy into harmonics (the third step).

This correspondence manifests itself in several features, as for instance in the time profile of HHG. This profile was obtained, in the two-level atom case, by applying a windowed Fourier transform in the dipole acceleration. The time-resolved spectra exhibit peaks at distinct population-transfer times t_1 . For both models, there is a single set of population-transfer times at the cutoff, which split into two in the plateau energy region. Such peaks become further apart as the harmonic energy decreases.

The single set of peaks at the cutoff corresponds, in the three-step model or in the two-level atom case, to

the maximal kinetic energy of the electron upon return or to the maximal energy difference between the adiabatic states, respectively. As the harmonic energy decreases, there are two possible sets of times for the electron to recombine, either from the continuum to the ground state [13] or from $|\phi_1^A(t)\rangle$ to $|\phi_0^A(t)\rangle$. These times are such that, in the former case, the harmonic energy is equal to the sum of the electron kinetic energy upon return and the ionization potential of the atom in question and, in the latter case, to the energy difference between the adiabatic states. All peaks in the windowed Fourier transform can be traced back to such population transfers, in analogy to studies performed within the three-step model framework.

For a monochromatic field, this pattern is periodic within half a cycle of the driving field, which is a consequence of the periodicity of the quantities involved, i.e., either of the kinetic energy of an electron upon

return or of the adiabatic energies. For bichromatic driving fields, this periodicity no longer holds. However, all peaks obtained in the time-resolved spectra can be associated with population-transfer times between adiabatic states. This is further confirmation of the three-step physical picture in the two-level atom case. Detailed studies of bichromatic fields were performed in [10].

Also for a two-level atom, analogously to the three-step model case, there is a phase difference between the harmonics and the incident driving field. This is due to the fact that there is a time delay between the first step, at t_0 , and the third step, at t_1 . The main difference between both cases is that, for a two-level atom, the phase is proportional to the field strength and not to the intensity. This is also true for other properties of high-order harmonics generated by a two-level atom, as for instance the cutoff law. Studies concerning this phase are in progress [18].

Another interesting property of HHG by a two-level atom is the existence of scaling laws, which give sets of parameters for which certain features, as for instance the number of harmonics in the spectra or their substructure, remain invariant. Such parameters are determined by $\gamma_1 = \omega/(2x_{10}E_0)$ or $\gamma_2 = \omega_{10}/(2x_{10}E_0)$, i.e., the ratio between the field and the atomic transition frequency to the Rabi frequency, respectively. In fact, we have shown that, even for completely different sets of field and atomic parameters, it is possible to obtain very similar spectra, as long as such quantities remain unchanged. On the other hand, even for small changes in E_0 , ω , ω_{10} , and x_{10} , if γ_1 and γ_2 do not remain invariant, the resulting spectra may be quite different.

Such criteria make it possible to extend the studies performed in this paper to more realistic situations. An example is a quantum well with $\omega_{10} \sim 10^{-4}$ a.u. and $x_{10} \sim 100$ a.u. subject to a field of strength $E_0 \sim 10^{-5}$ a.u. and frequency $\omega \sim 10^{-5}$ a.u. Under special conditions, the Hartree–Fock semiconductor Bloch equations, which describe transitions between two subbands in such systems, are formally identical to those describing the evolution of a two-level atom [9, 20, 22, 23]. These conditions are low doping intensity, equal effective masses in both subbands involved, parallel subbands, and not too wide wells. Thus, such systems may provide a concrete physical situation for which our results are applicable.

ACKNOWLEDGMENTS

We are grateful to V.P. Krainov for providing us a copy of his paper [7]. This work was supported in part by the Deutsche Forschungsgemeinschaft.

REFERENCES

1. Kuchiev, M.Yu., 1987, *Pis'ma Zh. Eksp. Teor. Fiz.*, **45**, 319 [1987, *JETP Lett.*, **45**, 404]; Corkum, P.B., 1993, *Phys. Rev. Lett.*, **71**, 1994; Kulander, K.C., Schafer, K.J., and Krause, J.L., 1993, in *Proceedings of the SILAP Conference*, Piraux, B. et al., Eds. (New York: Plenum); Lewenstein, M., Balcou, Ph., Ivanov, M.Yu., L'Huillier, A., and Corkum, P.B., 1994, *Phys. Rev. A*, **49**, 2117; Becker, W., Long, S., and McIver, J.K., 1990, *Phys. Rev. A*, **41**, 4112; 1994, *Phys. Rev. A*, **50**, 1540.
2. See, e.g., Sundaram, B. and Milonni, P., 1990, *Phys. Rev. A*, **41**, 6571; Plaja, L. and Roso-Franco, L., 1992, *J. Opt. Soc. Am. B*, **9**, 2210; Kaplan, A.E. and Shkolnikov, P.L., 1994, *Phys. Rev. A*, **49**, 6571; de Luca, S. and Fiordilino, E., 1996, *J. Phys. B*, **29**, 3277; Di Piazza, A., Fiordilino, E., and Mittleman, M., 2001, *Phys. Rev. A*, **64**, 013414.
3. Lenzner, M., Krüger, J., Sartania, S., Cheng, Z., Spielmann, Ch., Mourou, G., Kautek, W., and Krausz, F., 1998, *Phys. Rev. Lett.*, **80**, 4076.
4. Alon, O.E., Averbukh, V., and Moiseyev, N., 1998, *Phys. Rev. Lett.*, **80**, 3743; Hatsagorstyan, K.Z. and Keitel, C.H., 2001, *Phys. Rev. Lett.*, **86**, 12277; 2002, *J. Phys. B*, **35**, L175.
5. Alon, O.E., Averbukh, V., and Moiseyev, N., 2000, *Phys. Rev. Lett.*, **85**, 5218; Slepyan, G.Ya., Maksimentko, S.A., Kalosha, V.P., Gusakov, A.V., and Hermann, J., 2001, *Phys. Rev. A*, **63**, 053808.
6. Hay, N., Castillejo, M., de Nalda, R., Springate, E., Mendham, K.J., and Marangos, J.P., 2000, *Phys. Rev. A*, **61**, 053810; Hay, N., de Nalda, R., Halfmann, T., Mendham, K.J., Mason, M.B., Castillejo, M., and Marangos, J.P., 2000, *Phys. Rev. A*, **62**, 041803; Averbukh, V., Alon, O.E., and Moiseyev, N., 2001, *Phys. Rev. A*, **64**, 033411.
7. Krainov, V.P. and Mulyukov, Z.S., 1994, *Laser Phys.*, **4**, 544.
8. Gauthey, F.I., Garraway, B.M., and Knight, P.L., 1997, *Phys. Rev. A*, **56**, 3093.
9. Ivanov, M.Yu., Hawrylak, P., Haljan, P., Fortier, T., and Corkum, P.B. (unpublished).
10. Figueira de Morisson Faria, C. and Rotter, I., 2002, *Phys. Rev. A*, **66**, 013402.
11. Allen, L. and Eberly, J., 1975, *Optical Resonance and Two-Level Atoms* (New York: Wiley).
12. Rae, S.C., Burnett, K., and Cooper, J., 1994, *Phys. Rev. A*, **50**, 3438; Antoine, P., Piraux, B., and Maquet, A., 1995, *Phys. Rev. A*, **51**, R1750; Antoine, P., Piraux, B., Milošević, D.B., and Gajda, M., 1996, *Phys. Rev. A*, **54**, R1761.
13. Antoine, P., L'Huillier, A., and Lewenstein, M., 1996, *Phys. Rev. Lett.*, **77**, 1234; Figueira de Morisson Faria, C., Dörr, M., and Sandner, W., 1997, *Phys. Rev. A*, **55**, 3961; Antoine, Ph., Piraux, B., Milošević, D.B., and Gajda, M., 1997, *Laser Phys.*, **7**, 594.
14. Kan, C., Capjack, C.E., Rankin, R., and Burnett, N.H., 1995, *Phys. Rev. A*, **52**, R4336; Becker, W., Lohr, A., Long, S., McIver, J.K., Chichkov, B.N., and Welleghausen, B., 1997, *Laser Phys.*, **7**, 88.
15. Gaarde, M.B., Salin, F., Balcou, P., Schafer, K.J., Kulander, K.C., and L'Huillier, A., 1999, *Phys. Rev. A*,

- 59, 1367; Balcou, P., Dederichs, A.S., Gaarde, M.B., and L'Huillier, A., 1999, *J. Phys. B*, **32**, 2973.
16. Jung-Hoon Kim, Hyun Joon Shin, Dong Gun Lee, and Chang Hee Nam, 2000, *Phys. Rev. A*, **62**, 055402; Jung-Hoon Kim, Dong Gun Lee, Hyun Joon Shin, and Chang Hee Nam, 2001, *Phys. Rev. A*, **63**, 063403; Dong-Gun Lee, Jung-Hoon Kim, Kyung-Han Hong, and Chang Hee Nam, 2001, *Phys. Rev. Lett.*, **87**, 243902.
17. See, e.g., Bellini, M., Lynga, C., Tozzi, A., Gaarde, M.B., Hänsch, T.W., L'Huillier, A., and Wahlström, C.-G., 1998, *Phys. Rev. Lett.*, **81**, 297; Gaarde, M.B., Salin, F., Constant, E., Balcou, Ph., Schafer, K.J., Kulander, K.C., and L'Huillier, A., 1999, *Phys. Rev. A*, **59**, 1367; Balcou, P., Dederichs, A.S., Gaarde, M.B., and L'Huillier, A., 1999, *J. Phys. B*, **32**, 2973.
18. Figueira de Morisson Faria, C. and Rotter, I. (in preparation).
19. These oscillations are discussed in Garraway, B.M. and Vitanov, N.V., 1997, *Phys. Rev. A*, **55**, 4418 within a different context.
20. See, e.g., Birnir, B., Galdrikian, B., Grauer, R., and Sherwin, M., 1993, *Phys. Rev. B*, **47**, 6795(R).
21. Figueira de Morisson Faria, C., Fring, A., and Schrader, R., 2000, *J. Phys. B*, **33**, 1675.
22. Nikonov, D.E., Imamoglu, A., Butov, L.V., and Schmidt, H., 1997, *Phys. Rev. Lett.*, **79**, 4633; Krause, J.L., Reitze, D.H., Sanders, G.D., Kuznetsov, A.V., and Stanton, C.J., 1998, *Phys. Rev. B*, **57**, 9024.
23. See, e.g., Heyman, J.N., Craig, K., Sherwin, M.S., Campman, K., Hopkins, P.F., Fafard, S., and Gos-sard, C., 1994, *Phys. Rev. Lett.*, **72**, 2183; Galdrikian, B. and Birnir, B., 1996, *Phys. Rev. Lett.*, **76**, 3308.